Dentomaxillofacial Radiology (2015) 44, 20140428

birpublications.org/dmfr

RESEARCH ARTICLE

Influence of the artefact reduction algorithm of Picasso Trio CBCT system on the diagnosis of vertical root fractures in teeth with metal posts

[1]I S Q Bezerra, [1]F S Neves, [1]T V Vasconcelos, [2]G M B Ambrosano and [1]D Q Freitas

[1]Oral Radiology Area, Department of Oral Diagnosis, Piracicaba Dental School, State University of Campinas, Piracicaba, São Paulo, Brazil; [2]Department of Community Dentistry, Dental School of Piracicaba, State University of Campinas, Piracicaba, São Paulo, Brazil

Objectives: To assess the influence of the artefact reduction algorithm (AR) available on the Picasso Trio 3D® imaging system (Vatech, Hwaseong, Republic of Korea) on image quality [greyscale values, contrast-to-noise ratio (CNR) and artefact formation] and diagnosis of vertical root fractures (VRFs) in the teeth with intracanal metal posts.
Methods: 30 uniradicular teeth had their crowns removed and their roots endodontically treated to receive intracanal metal posts. In 20 teeth, both complete ($n = 10$) and incomplete ($n = 10$) VRFs were created. Each tooth was scanned twice, with and without AR activation. The mean and variation of greyscale values, as well as CNR, were calculated for all images. Subsequently, an evaluator compared the amount of artefact (cupping, white streaks and dark bands) in all images. Five evaluators rated for VRF presence using a five-point scale.
Results: Mean greyscale values and CNR were significantly decreased in images acquired with the AR. The usage of the algorithm promoted an overall reduction of image artefacts. Regarding the diagnosis of complete and incomplete VRFs, the use of the AR had an overall negative impact on specificity and accuracy.
Conclusions: While indeed reducing artefact formation, the use of the AR, instead of improving the impact on the diagnosis of VRFs in teeth with intracanal metal posts, had a negative impact on the diagnosis.
Dentomaxillofacial Radiology (2015) **44**, 20140428. doi: 10.1259/dmfr.20140428

Cite this article as: Bezerra ISQ, Neves FS, Vasconcelos TV, Ambrosano GMB, Freitas DQ. Influence of the artefact reduction algorithm of Picasso Trio CBCT system on the diagnosis of vertical root fractures in teeth with metal posts. *Dentomaxillofac Radiol* 2015; **44**: 20140428.

Keywords: tooth fractures; cone beam computed tomography; artefacts; diagnosis

Introduction

In daily dental practice, root fractures are a relatively common complication that may ultimately lead to removal of the damaged tooth. Studies that investigated the reasons for tooth extraction reported that 7.7–32.1% of such procedures were secondary to root fractures.[1–3] Vertical root fractures (VRFs), which run oblique to the long axis of the tooth, normally are caused by eccentric occlusal forces, external trauma, successive restorative dentistry, excessive pressure during endodontic treatment, poorly designed intracanal posts, inappropriate selection of teeth as abutments for prosthetic bridges or parafunctional habits.[4–7] Early detection of fractured roots is vital for preventing damage to the periodontium and for a quick treatment start.[5,8]

CBCT is gradually becoming the standard for diagnostic imaging in dentistry.[9] The limitations imposed by two-dimensional images in the assessment of endodontic conditions are usually being replaced by the three-dimensionality of CBCT, which has proved itself

Correspondence to: Dr Deborah Queiroz Freitas. E-mail: deborahq@unicamp.br
Received 12 December 2014; revised 3 February 2015; accepted 11 March 2015

useful for assessing the extent of periapical lesions and their relationship with nearby anatomical structures, as well as for visualizing complex root canal anatomy and for root fracture detection.[10,11]

Studies have demonstrated the efficacy of CBCT in the diagnosis of root fractures in teeth without intracanal filling materials.[5,12,13] If filling materials are present, the reports are inconclusive, but there seems to be some level of compromise in diagnostic accuracy.[8,12,14,15] In CT imaging of cases in which high-density intracanal materials such as gutta percha or metal posts are present, there will be artefact formation. Artefacts affect image quality and may increase difficulty of root fracture diagnosis substantially.[4,12,15–18] In teeth with intracanal fillings, artefacts occur owing to differences in the attenuation and absorption of X-ray beams by high-density material physics that cause beam-hardening phenomenon. The resulting image is altered by hypodense bands (dark bands), hyperdense striations (white streaks) and distortion of metal objects (cupping artefacts), which can all interfere with fracture detection and may lead to false-positive results.[8,14,19,20]

Recently, an artefact reduction algorithm (AR) that applies algorithms during image reconstruction has been introduced by some CBCT systems. However, few studies have evaluated this tool, and the results are inconclusive as to its influence on the final image quality.[21–23] When evaluated for root fracture diagnosis in teeth filled with gutta-percha, the use of an AR led to decreased diagnostic sensitivity and specificity.[4] Additionally, no differences were observed in the detection of simulated periodontal and peri-implant vestibular defects with or without the use of an AR.[24]

Thus, the benefits of using an AR are not well established, and studies to date have used either subjective or objective evaluations but not the two forms of assessments combined. In addition, studies that evaluate the usefulness of AR in the detection of root fractures in teeth with intracanal metal posts, which happen relatively often, are missing. Therefore, this study aimed to evaluate the influence of AR on image quality [greyscale values, contrast-to-noise ratio (CNR) and artefact formation] and on the diagnosis of VRFs in teeth with intracanal metal posts.

Methods and materials

The local research ethics committee approved this work without restrictions (Protocol 650 253).

Sample selection and preparation

30 uniradicular human teeth were selected and prepared according to the methodology applied by Neves et al.[15] In short, dental crowns were removed at the cementoenamel junction, and root canals were prepared endodontically with the rotary system Mtwo® NiTi (VDW, Munich, Germany). Subsequently, preparations for metal post placement were performed with a drill (# 2, Exacto; Angelus, Londrina, Brazil) at low speed up to two-thirds the length of the root canal.

For fracture induction, 20 roots were randomly selected and placed in an acrylic block, which was positioned on a universal testing machine (model 4411; Instron® Corporation, Canton, MA), and fractures were induced by applying a 500 N load at a speed of 1 mm min^{-1}. The process of fracture induction was confirmed under visual inspection and transillumination with an light emitting diode photopolymerization unit (Ultra-Lume 5; Ultradent Products Inc., South Jordan, UT). 10 roots were completely fractured (with fragment displacement, but without fragment separation or need for gluing), and the remaining 10 roots were incompletely fractured (without fragment displacement). The other 10 roots were not fractured (control group). The knowledge of the condition of each root was used as the gold standard to evaluate the performance of VRF diagnosis.

Image acquisition

For image acquisition, the roots were removed from the acrylic block and placed in the left and right second premolar alveoli of macerated mandible, and customized Co–Cr metal posts were placed in all roots. The mandible and roots were positioned at the centre of a cylindrical plastic box completely filled with water in order to simulate soft-tissue coverage. Three human vertebrae (C1, C2 and C3) were placed in the same container dorsally to the mandible to simulate *in vivo* X-ray beam attenuation and dispersion.[15,25]

CBCT scans were performed with the Picasso Trio imaging device (Vatech, Hwaseong, South Korea) with the following exposure protocol: 90 kVp; 5 mA; field of view of 8 × 5 cm; and 0.2-mm voxel. Two acquisitions were made for each root, with and without AR activation (Figure 1).

Image assessment

All evaluations were conducted using a 19-inch liquid crystal display monitor (1366 × 768 pixels spatial resolution, 32-bit) in a quiet environment with low ambient lighting.

Greyscale variables: In this evaluation, the mean greyscale values, the greyscale variation and the CNR were obtained.

Greyscale values were determined objectively with the aid of ImageJ (National Institutes of Health, Bethesda, MD) by an experienced examiner. In the axial view, a circular region of interest (ROI) was selected encompassing the central region of the tooth but not involving the surrounding tissues, thereby allowing the verification of greyscale values for artefacts formed over the root. The ROI was set at the same size (3 mm in diameter) for all analyses. ImageJ provided a histogram with standard deviation, mean greyscale values and maximum and minimum greyscale values for each given ROI (Figure 2). Measurements were performed at the apical, middle and cervical thirds of each root (Figure 3),

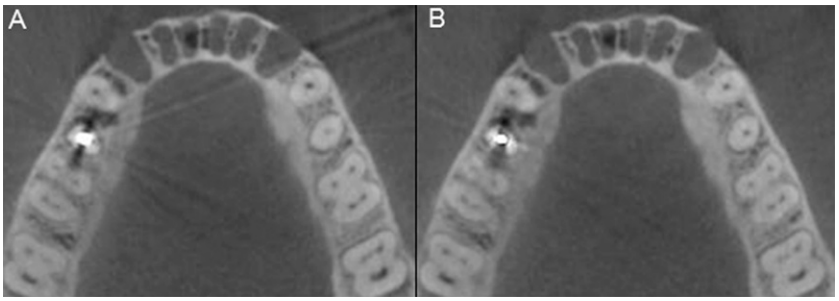

Figure 1 Image acquisition. (a) Without artefact reduction algorithm (AR) and (b) with AR.

and the average of the three measures was used as the mean greyscale value. The slice representative of the apical third corresponded to the most apical slice in which the post was seen, while the slice representative of the cervical third was the most cervical slice in which the post could be identified. The slice representing the middle third was the one in the middle of the interval formed by the other two.

A similar evaluation was performed for the control ROI, which was set to the mid-posterior region of the volume and had the same size of the ROI over the root (Figure 2). For the control ROI, an ImageJ histogram also provided the same data mentioned above. The CNR was calculated according to the formula:

$$CNR = \frac{Sa - Sb}{\sigma b}$$

in which Sa is the mean greyscale value for the ROI over the root as provided by the histogram, Sb is the mean greyscale value for the control ROI and σb corresponds to the standard deviation for the control ROI.[21,22] This analysis was conducted for all images, both with and without the use of AR.

The range of greyscale variation was determined by the difference of the maximum and minimum values provided by the histogram of the ROIs from the roots.

After 60 days, 20% of the sample was reviewed to evaluate the reproducibility of greyscale values.

Artefact formation: An examiner quantified artefact formation in images acquired with AR activated, using the same axial slices in which greyscale values were quantified. The artefacts assessed were cupping, dark bands (formed mainly in the mesial and distal regions of the root) and white streaks (formed from the post and extending throughout the image). Concomitantly, the same axial slice of the same root with and without the AR was visualized. The changes in artefact production in the images with the AR activated were assessed, using as reference the correspondent image without the AR. Regarding the image with AR activation, the examiner marked one of the following answers: there was no change, there was reduction or there was an increase in the amount of artefact formation.

This evaluation was repeated in 20% of the sample after 60 days.

Vertical root fracture diagnosis: Five oral radiologists who had at least 4 years experience with CBCT imaging were calibrated to analyse the images and rate each root for the presence of VRF using a five-point scale in which (1) VRF was definitely absent, (2) VRF was probably absent, (3) uncertain, (4) VRF was probably present and (5) VRF was definitely present. The examiners were blinded and worked independently using the native Ez3D software package (Vatech, E-WOO Technology, Republic of Korea). Image observation could be conducted in all tomographic planes; brightness,

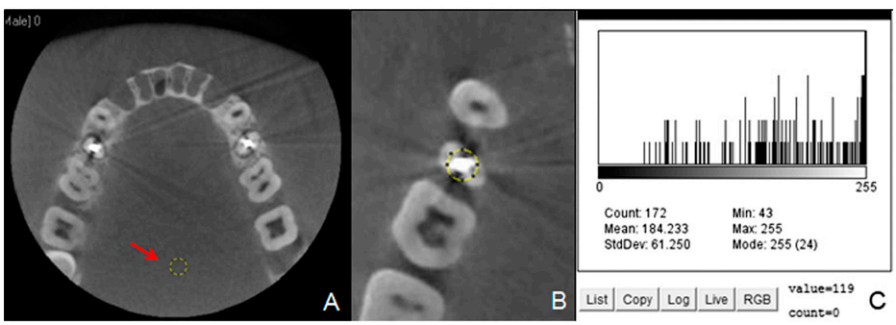

Figure 2 Selection of the region of interest (ROI) in ImageJ (National Institutes of Health, Bethesda, MD) to determine the mean and variation of greyscale values and the contrast-to-noise ratio. (a) ImageJ screen capture showing the ROI to evaluate the area selected as control (circle indicated by arrow). (b) ROI to evaluate the area selected as artefact (circle). (c) ImageJ histogram showing greyscale count (Count), mean (Mean), standard deviation (StdDev), Minimum (Min) and maximum (Max) values and mode (Mode) for the ROI.

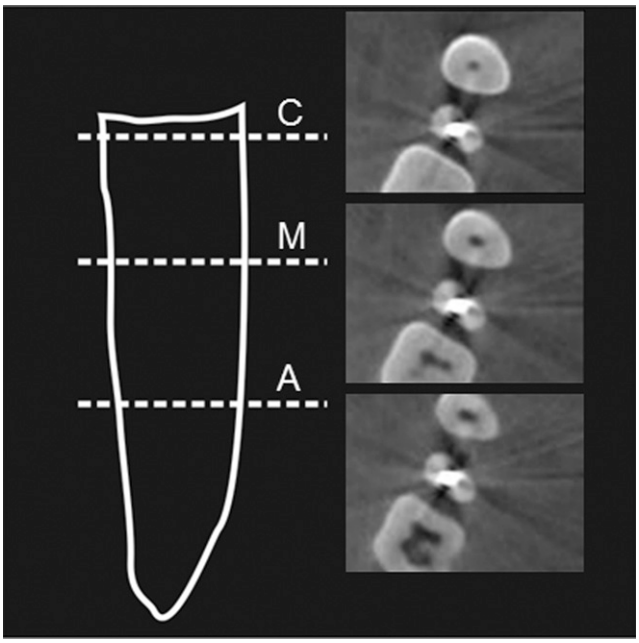

Figure 3 Areas of region of interest selection in the apical (A), middle (M) and cervical (C) thirds of the root.

contrast and zoom could be changed at each examiner's discretion. After 30 days, 20% of the sample was reassessed by the five observers to calculate intraexaminer agreement.

Statistical analysis

Comparison of the results obtained from the subjective assessment against the gold standard was carried out by analysing the receiver operating characteristic (ROC) curve. Values for sensitivity, specificity and accuracy were also calculated using Rating 3 as the cut-off point. These analyses were performed in a web-based calculator for ROC curves (http://www.rad.jhmi.edu/jeng/javarad/roc/JROCFITi.html).[26] These values were calculated for each observer for each image modality (image with and without AR). The paired *t*-test was used for comparing results from images with and without AR activation regarding the greyscale variables (mean greyscale values, greyscale variation and CNR), the areas under the ROC curve and the diagnostic tests (sensitivity, specificity and accuracy). The reproducibility of greyscale values was assessed by intraclass correlation coefficient. Intraexaminer agreement of artefact formation and intra- and interexaminer agreement of VRF diagnosis was assessed by weighted kappa and interpreted based on Landis and Koch.[27] Analyses were performed with SAS® System release 9.2—TS Level 2 M0 (SAS Institute Inc., Cary, NC), with a significance level of 5%. For every studied variable, the powder of the tests was superior to 0.8.

Artefact formation was evaluated by descriptive statistics.

Results

Greyscale variables

Table 1 shows the values obtained for greyscale variables in the objective assessment. According to the paired *t*-test, there was a significant reduction in the mean greyscale values when AR was used ($p = 0.002$) and CNR also varied significantly ($p = 0.000$), showing higher values when AR was not used. Greyscale variation did not show a statistically significant difference.

Artefact formation

Assessment of artefact formation is shown in Table 2. There was an overall reduction in artefact formation in images in which AR was activated when compared with images without AR, especially for cupping and dark bands.

Vertical root fracture diagnosis

Table 3 shows the values for areas under the ROC curve (Az) and for the diagnostic tests with and without AR in roots with incomplete and complete VRFs. In general, values were lower with AR. The paired *t*-test indicated that specificity and accuracy were significantly lower with the use of AR. This pattern was repeated in teeth with complete and incomplete VRFs.

Intra- and interexaminer agreement

The intraclass correlation coefficient showed excellent reproducibility of greyscale values (0.98 without AR and 0.97 with AR). The weighted kappa also indicated that the intraexaminer agreement regarding artefact formation was excellent (0.89). However, the intra- and interexaminer agreement concerning VRF diagnosis with and without AR activation ranged from slight to fair, according to the weighted kappa (Table 4).

Table 1 Mean (± standard deviation) of the variables analysed in the objective assessment

Variables analyzed	*With artefact reduction algorithm*	*Without artefact reduction algorithm*	p-*value*[a]
Mean greyscale values	173.46 (11.35)	182.70 (14.58)	0.002
Contrast-to-noise ratio	37.92 (6.53)	42.58 (6.50)	0.000
Greyscale variation	226.43 (31.64)	221.37 (22.02)	0.309

[a]According to *t*-test.

Table 2 Assessment of artefact formation in images acquired with artefact reduction algorithm (AR) compared with those obtained without AR algorithm (%)

Artefact formation	*White streaks*	*Dark bands*	*Cupping*
Unaltered	36.66	10	10
Reduction	46.67	70	80
Increase	16.67	20	10

Discussion

High-density root-filling materials can create artefacts in tomographic images and have been shown to increase the difficulty of root fracture diagnosis.[13,17,18] The influence of AR has been studied; nevertheless, our literature review showed that only one study evaluated its influence on the diagnosis of root fractures.[4] That study, however, used root canals filled with gutta-percha, a material known to produce fewer artefacts than do metal posts.[28] Given the paucity of research regarding the issue, we pursued the task of scrutinizing an AR offered by a commercially available CBCT system (Picasso Trio 3D) concerning its ability to ease VRF diagnosis in teeth with intracanal metal posts. To do that, we combined objective (image quality) and subjective (artefact formation and VRF diagnosis) assessments and were, to our knowledge, the first group to do so in this particular topic.

Objective assessments of images obtained with AR activated have been performed already.[21,22] By analysing mean greyscale values in a similar CBCT equipment, both with and without the use of AR, Bechara et al[22] showed that this value was significantly lower with the use of such tool, corroborating the results of our study. On the other hand, Bechara et al[21] observed a significant increase in mean greyscale values using the AR in the presence of metal, while values were reduced in the absence of metal. However, both reports used phantoms and assessed different areas, while our study simulated a clinical condition. Physiological bone structures can cause significant radiation scattering, which cannot be assessed in studies using homogeneous phantoms.[23] Parsa et al[23] also calculated mean greyscale values to assess AR use in sites adjacent to dental implants. By comparing the areas of interest before and after implant insertion, they reported a significant increase in mean greyscale values after surgery and, when comparing the images obtained with and without the use of the AR, found out that there was no change in greyscale values with the tool activated. Thus, it seems that the influence of the tool may vary depending on the particularities of a given study: if a phantom is used, if a clinical condition is simulated, which artefact-inducing material is used, and if specific materials are employed.

Assessments on artefact formation could explain the higher mean greyscale values found in images obtained without AR activation, which means that the images obtained were perceived as brighter on ImageJ. We postulate that this was owing to the increased cupping in images without AR activation, which may constitute a significant hyperdense portion of the ROI.

Increase in CNR seems to improve image quality.[21,29] However, the results of this study showed a decrease of this ratio when AR was used, while Bechara's group[21,22] have reported that the CNR is increased with AR use. In addition, one must consider that these studies were conducted in phantoms and, despite satisfactory standardization, evaluate variables that may not be present in clinical situations.

Difficulties in the diagnosis of root fractures in roots filled with high-density materials owing to artefact formation is one well-established problem in the literature.[7,8,12,14,15,17,18] The AR has emerged as an alternative to control artefact formation and thus increase diagnostic certainty. However, we could not confirm this hypothesis, as some have already reported.[4,24] When assessing two different imaging systems with AR (Picasso Master 3D and Planmeca ProMax® 3D Max; Planmeca Oy, Helsinki, Finland) regarding root fracture diagnosis in teeth filled with gutta percha, Bechara et al[4] reported overall inferior results with the use of the tool. By using an AR in an attempt to improve the detection of peri-implant and periodontal defects, Kamburoglu et al[24] were also unable to deliver promising conclusions.

One can perceive how more challenging it is to evaluate images tainted with artefacts caused by metal in comparison with those caused by gutta-percha by comparing the values found in this study and in the work mentioned above, since our numbers were lower regardless of AR use.[4] That group judged that the images they obtained were suitable for root

Table 3 Mean values (± standard deviation) for the area under the receiver operating characteristic curve (Az) and for the diagnostic tests (sensitivity, specificity and accuracy) with the artefact reduction algorithm (W/AR) and without the artefact reduction algorithm (Wo/AR) considering incomplete and complete vertical root fractures (VRFs)

Type of fracture	*Artefact reduction algorithm*	*Az*	*Sensitivity*	*Specificity*	*Accuracy*
Incomplete VRF	W/AR	0.470 (0.15)	0.383 (0.19)	0.433 (0.10)	0.408 (0.12)
	Wo/AR	0.514 (0.06)	0.450 (0.12)	0.583 (0.19)	0.516 (0.08)
	p-value	0.332	0.637	0.028[a]	0.037[a]
Complete VRF	W/AR	0.496 (0.12)	0.483 (0.22)	0.433 (0.10)	0.458 (0.11)
	Wo/AR	0.542 (0.06)	0.483 (0.11)	0.583 (0.19)	0.533 (0.06)
	p-value	0.344	0.511	0.021[a]	0.031[a]

[a]Significant difference according to *t*-test.

Table 4 Intra- and interexaminer agreement intervals of evaluation concerning vertical root fractures diagnosis

Artefect reduction algorithm	*Intraexaminer agreement*	*Interexaminer agreement*
With	0–0.4	0.05–0.36
Without	0–0.31	0.01–0.38

fracture diagnosis given that values for the areas under the ROC curves (Az) were >0.5. This idea does not find support in our results since our Az values were slightly >0.5 without AR and lower with AR; therefore, CBCT seems scarcely a promising method for fracture detection in the presence of metal posts owing to the higher amount of artefacts formed. Neves et al,[15] while evaluating the diagnosis of incomplete root fractures in the presence of different intracanal filling materials, also reached Az values <0.5 when a metal post was used independently of the several protocols used in that study.

Several methods have been devised to control artefact formation in tomographic images: increasing kilovolt peak (kVp), for example, seems to enhance image quality.[21,30] Bechara et al[16] observed that doubling up the number of base images during acquisition promoted a significant decrease in the number of false-positive diagnosis of root fractures, thereby being an option to reduce artefacts caused by high-density objects. On the other hand, Neves et al[15] also increased the number of base images for diagnosing root fractures in the presence of metal posts but observed no improvement and concluded that such an approach does not help with root fracture diagnosis. One must bear in mind that doubling up base images or increasing kVp also increases the radiation dose that patient receive.[31] Thus, cases must be evaluated carefully and individually so that acquisition parameters are chosen to provide cost-effectiveness and avoid radiation overdosing.

Fracture width must be taken into account at the time of diagnosis since complete fractures are more easily identified in CBCT scans than in incomplete ones; a finding ratified by the present study and other studies.[5,8,15] It is therefore paramount to be judicious when inducing root fractures for experimental purposes. Some studies have induced root fractures by hammering, with a screwdriver or a screw, and then repositioning and gluing the fragments.[7,13,14,17,19] According to Patel et al,[8] it is not possible to create an incomplete fracture (<150 μm) with such techniques; the resulting fractures would be much larger (>200 μm) and more easily detectable. We chose to use a universal testing machine so that the force applied to the roots was precisely controlled and incomplete fracture creation could be reproducible, as some have performed before.[5,8,15]

Artefacts are caused by discrepancies between the physical object or body being scanned and the mathematical calculations used to create three-dimensional reconstructions of that object or body, and can lead to diagnostic errors.[20] According to Patel et al,[8] tomographic images with artefacts may produce low values regarding intra- and interexaminer diagnostic agreement. We found low values for inter- and intraexaminer agreement in the present study, as have other studies,[4,8,15] where agreement levels obtained ranged from poor to moderate. We agree with the suppositions proposed by these authors that these results are related to excessive artefact formation, which makes interpretation of the areas of interest much more difficult.

According to the SEDENTEXCT guidelines[32] and the European Society of Endodontology[33] guidelines, CBCT examinations are only indicated in selected cases when intraoral radiographs do not provide adequate information for management, considering the higher doses of radiation and the higher cost of the first examination when compared with that of the last one. As conventional radiographs and CBCT images have been already compared for root fracture diagnosis in the literature,[34–38] we decided not to include periapical radiography, since the main objective of the study was to evaluate the influence of the CBCT AR in the detection of complete and incomplete root fractures. The assessment of incomplete root fractures is a difficult diagnostic task; in this sense, even in CBCT examinations of teeth with clinical signs of root fracture, the fracture lines may not be visualized.[39]

It is important to take note that this was, to our knowledge, the first study evaluating the AR application as a possible aid to the diagnosis of root fractures in root canals bearing metal posts, but these results are related to that diagnostic task and the AR of the Picasso Trio scanner. More studies should be conducted to obtain evidence regarding other clinical situations that may or may not support the regular use of this tool, since AR use increases reconstruction time.

Conclusion

While the AR algorithm analysed in this study reduced artefact formation, it had a negative impact on diagnosis of complete or incomplete VRFs in root canals with intracanal metal posts. Based on our results and considering that AR use increases image reconstruction time, the regular AR application is not recommended in this specific clinical condition.

References

1. Chen SC, Chueh LH, Hsiao CK, Wu HP, Chiang CP. First untoward events and reasons for tooth extraction after nonsurgical endodontic treatment in Taiwan. *J Endod* 2008; **34**: 671–4. doi: 10.1016/j.joen.2008.03.016
2. Fuss Z, Lustig J, Tamse A. Prevalence of vertical root fractures in extracted endodontically treated teeth. *Int Endod J* 1999; **32**: 283–6.
3. Majorana A, Pasini S, Bardellini E, Keller E. Clinical and epidemiological study of traumatic root fractures. *Dent Traumatol* 2002; **18**: 77–80.
4. Bechara B, Alex McMahan C, Moore WS, Noujeim M, Teixeira FB, Geha H. Cone beam CT scans with and without artefact reduction in root fracture detection of endodontically treated teeth. *Dentomaxillofac Radiol* 2013; **42**: 20120245. doi: 10.1259/dmfr.20120245
5. Brady E, Mannocci F, Brown J, Wilson R, Patel S. A comparison of cone beam computed tomography and periapical radiography for the detection of vertical root fractures in non-endodontically treated teeth. *Int Endod J* 2014; **47**: 735–46. doi: 10.1111/iej.12209
6. Cohen S, Blanco L, Berman L. Vertical root fractures: clinical and radiographic diagnosis. *J Am Dent Assoc* 2003; **134**: 434–41.
7. Melo SL, Bortoluzzi EA, Abreu M Jr, Corrêa LR, Corrêa M. Diagnostic ability of a cone-beam computed tomography scan to assess longitudinal root fractures in prosthetically treated teeth. *J Endod* 2010; **36**: 1879–82. doi: 10.1016/j.joen.2010.08.025
8. Patel S, Brady E, Wilson R, Brown J, Mannocci F. The detection of vertical root fractures in root filled teeth with periapical radiographs and CBCT scans. *Int Endod J* 2013; **46**: 1140–52. doi: 10.1111/iej.12109
9. Scarfe WC, Farman AG. What is cone-beam CT and how does it work? *Dent Clin North Am* 2008; **52**: 707–30. doi: 10.1016/j.cden.2008.05.005
10. Patel S. New dimensions in endodontic imaging: part 2. Cone beam computed tomography. *Int Endod J* 2009; **42**: 463–75. doi: 10.1111/j.1365-2591.2008.01531.x
11. Patel S, Dawood A, Ford TP, Whaites E. The potential applications of cone beam computed tomography in the management of endodontic problems. *Int Endod J* 2007; **40**: 818–30.
12. Khedmat S, Rouhi N, Drage N, Shokouhinejad N, Nekoofar MH. Evaluation of three imaging techniques for the detection of vertical root fractures in the absence and presence of gutta-percha root fillings. *Int Endod J* 2012; **45**: 1004–9. doi: 10.1111/j.1365-2591.2012.02062.x
13. Özer SY. Detection of vertical root fractures by using cone beam computed tomography with variable voxel sizes in an *in vitro* model. *J Endod* 2011; **37**: 75–9. doi: 10.1016/j.joen.2010.04.021
14. Hassan B, Metska ME, Ozok AR, van der Stelt P, Wesselink PR. Comparison of five cone beam computed tomography systems for the detection of vertical root fractures. *J Endod* 2010; **36**: 126–9. doi: 10.1016/j.joen.2009.09.013
15. Neves FS, Freitas DQ, Campos PS, Ekestubbe A, Lofthag-Hansen S. Evaluation of cone-beam computed tomography in the diagnosis of vertical root fractures: the influence of imaging modes and root canal materials. *J Endod* 2014; **40**: 1530–6. doi: 10.1016/j.joen.2014.06.012
16. Bechara B, McMahan CA, Nasseh I, Geha H, Hayek E, Khawam G, et al. Number of basis images effect on detection of root fractures in endodontically treated teeth using a cone beam computed tomography machine: an *in vitro* study. *Oral Surg Oral Med Oral Pathol Oral Radiol* 2013; **115**: 676–81. doi: 10.1016/j.oooo.2013.01.026
17. Junqueira RB, Verner FS, Campos CN, Devito KL, do Carmo AM. Detection of vertical root fractures in the presence of intracanal metallic post: a comparison between periapical radiography and cone-beam computed tomography. *J Endod* 2013; **39**: 1620–4. doi: 10.1016/j.joen.2013.08.031
18. Melo SL, Haiter-Neto F, Correa LR, Scarfe WC, Farman AG. Comparative diagnostic yield of cone beam CT reconstruction using various software programs on the detection of vertical root fractures. *Dentomaxillofac Radiol* 2013; **42**: 20120459. doi: 10.1259/dmfr.20120459
19. Hassan B, Metska ME, Ozok AR, van der Stelt P, Wesselink PR. Detection of vertical root fractures in endodontically treated teeth by a cone beam computed tomography scan. *J Endod* 2009; **35**: 719–22. doi: 10.1016/j.joen.2009.01.022
20. Schulze R, Heil U, Gross D, Bruellmann DD, Dranischnikow E, Schwanecke U, et al. Artefacts in CBCT: a review. *Dentomaxillofac Radiol* 2011; **40**: 265–73. doi: 10.1259/dmfr/30642039
21. Bechara B, McMahan CA, Geha H, Noujeim M. Evaluation of a cone beam CT artefact reduction algorithm. *Dentomaxillofac Radiol* 2012; **41**: 422–8. doi: 10.1259/dmfr/43691321
22. Bechara BB, Moore WS, McMahan CA, Noujeim M. Metal artefact reduction with cone beam CT: an *in vitro* study. *Dentomaxillofac Radiol* 2012; **41**: 248–53. doi: 10.1259/dmfr/80899839
23. Parsa A, Ibrahim N, Hassan B, Syriopoulos K, van der Stelt P. Assessment of metal artefact reduction around dental titanium implants in cone beam CT. *Dentomaxillofac Radiol* 2014; **43**: 20140019. doi: 10.1259/dmfr.20140019
24. Kamburoglu K, Kolsuz E, Murat S, Eren H, Yüksel S, Paksoy CS. Assessment of buccal marginal alveolar peri-implant and periodontal defects using a cone beam CT system with and without the application of metal artefact reduction mode. *Dentomaxillofac Radiol* 2013; **42**: 20130176. doi: 10.1259/dmfr.20130176
25. Katsumata A, Hirukawa A, Okumura S, Naitoh M, Fujishita M, Ariji E, et al. Effects of image artifacts on gray-value density in limited-volume cone-beam computerized tomography. *Oral Surg Oral Med Oral Pathol Oral Radiol Endod* 2007; **104**: 829–36.
26. Eng J. ROC analysis: web-based calculator for ROC curves. Baltimore, MD: Johns Hopkins University. [Updated 19 March 2014.] Available from: http://www.jrocfit.org/
27. Landis JR, Koch GG. The measurement of observer agreement for categorical data. *Biometrics* 1977; **33**: 159–74.
28. Klinke T, Daboul A, Maron J, Gredes T, Puls R, Jaghsi A, et al. Artifacts in magnetic resonance imaging and computed tomography caused by dental materials. *PLoS One* 2012; **7**: e31766. doi: 10.1371/journal.pone.0031766
29. Suomalainen A, Kiljunen T, Käser Y, Peltola J, Kortesniemi M. Dosimetry and image quality of four dental cone beam computed tomography scanners compared with multislice computed tomography scanners. *Dentomaxillofac Radiol* 2009; **38**: 367–78. doi: 10.1259/dmfr/15779208
30. Oliveira ML, Freitas DQ, Ambrosano GM, Haiter-Neto F. Influence of exposure factors on the variability of CBCT voxel values: a phantom study. *Dentomaxillofac Radiol* 2014; **43**: 20140128. doi: 10.1259/dmfr.20140128
31. Lofthag-Hansen S, Thilander-Klang A, Gröndahl K. Evaluation of subjective image quality in relation to diagnostic task for cone beam computed tomography with different fields of view. *Eur J Radiol* 2011; **80**: 483–8. doi: 10.1016/j.ejrad.2010.09.018
32. SEDENTEXCT guidelines. Safety and efficacy of a new and emerging dental X-ray modality. Radiation protection no. 172: cone beam CT for dental and maxillofacial radiology (evidence-based guidelines). 2012. [Updated March 2012.] Available from: http://www.sedentexct.eu/files/radiation_protection_172.pdf
33. European Society of Endodontology; Patel S, Durack C, Abella F, Roig M, Shemesh H, Lambrechts P, et al. European Society of Endodontology position statement: the use of CBCT in endodontics. *Int Endod J* 2014; **47**: 502–4. doi: 10.1111/iej.12267

34. Wenzel A, Haiter-Neto F, Frydenberg M, Kirkevang LL. Variable-resolution cone-beam computerized tomography with enhancement filtration compared with intraoral photostimulable phosphor radiography in detection of transverse root fractures in an *in vitro* model. *Oral Surg Oral Med Oral Pathol Oral Radiol Endod* 2009; **108**: 939–45. doi: 10.1016/j.tripleo.2009.07.041
35. Varshosaz M, Tavakoli MA, Mostafavi M, Baghban AA. Comparison of conventional radiography with cone beam computed tomography for detection of vertical root fractures: an *in vitro* study. *J Oral Sci* 2010; **52**: 593–7.
36. Kamburoğlu K, Murat S, Yüksel SP, Cebeci AR, Horasan S. Detection of vertical root fracture using cone-beam computerized tomography: an *in vitro* assessment. *Oral Surg Oral Med Oral Pathol Oral Radiol Endod* 2010; **109**: e74–81. doi: 10.1016/j.tripleo.2009.09.005
37. Wang P, Yan XB, Lui DG, Zhang WL, Zhang Y, Ma XC. Detection of dental root fractures by using cone-beam computed tomography. *Dentomaxillofac Radiol* 2011; **40**: 290–8. doi: 10.1259/dmfr/84907460
38. da Silveira PF, Vizzotto MB, Liedke GS, da Silveira HL, Montagner F, da Silveira HE. Detection of vertical root fractures by conventional radiographic examination and cone beam computed tomography—an *in vitro* analysis. *Dent Traumatol* 2013; **29**: 41–6. doi: 10.1111/j.1600-9657.2012.01126.x
39. Kajan ZD, Taromsari M. Value of cone beam CT in detection of dental root fractures. *Dentomaxillofac Radiol* 2012; **41**: 3–10. doi: 10.1259/dmfr/25194588